Inorganica Chimica Acta, *109* (1985) 193–197

Decomposition of Water by Cerium Oxide of δ-Phase

KIYOSHI OTSUKA*, MASAHARU HATANO and AKIRA MORIKAWA

Department of Chemical Engineering, Tokyo Institute of Technology, Ookayama, Meguro-ku, Tokyo 152, Japan

Received November 20, 1984

Abstract

Reduced cerium dioxide (CeO_{2-x}) can reduce water, producing hydrogen at $\geqslant$298 K. Kinetic studies were focused on the stoichiometric reaction of δ-phase cerium oxide ($CeO_{1.818}$) with water vapor. Different activation energies of 18.1 and 33.4 kJ mol^{-1} were observed for the reactions at the temperature ranges above and below *ca.* 453 K, respectively. Rate equations observed in the two temperature ranges were also different. These results strongly suggest that the rate-determining steps are different between the two temperature ranges. Rapid oxygen exchange observed between $H_2{}^{18}O$ and lattice oxygen in cerium oxide of δ-phase at $\geqslant$298 K indicated that neither the adsorption of water molecules nor the diffusion of oxygen ions in the bulk of the oxide can be the rate-determining step. H_2–D_2 exchange occurred rapidly at 373 K compared to the rate of water decomposition, suggesting that the recombination of hydrogen atoms on the surface is not rate-determining either. A tentative reaction mechanism was proposed to explain the results of the kinetic studies. The rate-determining step at high temperatures (>453 K) is the reduction of OH^- by the six-coordinated Ce^{3+} which is present in the nonstoichiometric cerium oxide, while that at low temperatures (<453 K) is the subsequent reduction of H^+ by the seven-coordinated Ce^{3+}.

Introduction

The production of hydrogen from water applying a solid–gas reaction has recently been studied and developed [1–5]. There are many metal oxides which decompose water thermodynamically in the reduced state, producing hydrogen accompanying regeneration of the original higher-valent metal oxides. Preliminary experiments showed that CeO_2 was the only stable metal oxide of the lanthanide elements which is reduced at <873 K and the reduced state decomposes water. The decomposition of water by reduced cerium dioxide (CeO_{2-x}) has been demonstrated to occur rapidly at <473 K [5]. However, the detailed chemistry and kinetics of the reaction have not yet been reported.

There has been considerable interest in recent years in the oxides of the rare earths Ce, Pr, and Tb, all of which can be reduced from the dioxide RO_2 (R = rare earth) having the fluorite structure, to compositions over a range extending to R_2O_3, which has the A-type or C-type sesquioxide structure [6]. In each of these systems the nonstoichiometric defects are believed to be oxygen vacancies. In the range of compositions between RO_2 and R_2O_3, at relatively low temperatures ($T \leqslant 773$ K), there exists a number of ordered phases which are generally believed to form a homologous series of the type R_nO_{2n-2}, where n can take on a number of integer values [7]. In the CeO_{2-x} system, Bevan and Kordis [8] have revealed that there are three distinct intermediate phases at $CeO_{1.714}(\iota)$, $CeO_{1.778}(\zeta)$ and $CeO_{1.818}(\delta)$ which correspond to n = 7, 9 and 11 in the formula R_nO_{2n-2}. Figure 1 shows the phase diagram proposed by Bevan and Kordis [8]. Ray and Nowick [9] have shown that there is another phase at $CeO_{1.800}(\epsilon)$ (n = 10). These phases are thought to be formed by ordering of oxygen vacancies in one way or another, and at high temperatures they transform to fluorite-type structures in which the vacancies are disordered.

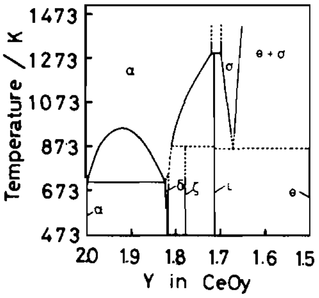

Fig. 1. Phase diagram of cerium oxides according to Bevan and Kordis [8].

---

*Author to whom correspondence should be addressed.

0020-1693/85/$3.30

High anion mobility in these nonstoichiometric oxides RO_{2-x} is well recognized [8, 10–14]. The most striking example is the CeO_{2-x} system in which reoxidation takes place even at room temperature [8, 11]. Ray and Nowick [11] reported detailed kinetic studies on the oxidation of single crystals of CeO_{2-x} by oxygen at temperatures 296–342 K. They suggested that the rate-controlling mechanism was the phase-boundary reaction between the reduced phase and the metastable α'-phase which was distinguished from the fully oxidized $CeO_2(\alpha)$. Under these circumstances, it is particularly interesting to elucidate the mechanism of reoxidation of CeO_{2-x} by water. The purpose of this work is to investigate the fundamental behavior in the oxidation of the partially reduced-cerium dioxide (CeO_y, y is average O/Ce ratio) with water vapor by kinetic studies on the reaction. The oxygen-exchange between $H_2{}^{18}O$ and CeO_y and H_2–D_2 exchange on CeO_y will also be investigated to get information about the reaction mechanism.

Experimental

Materials

The CeO_2 used was a reagent-grade powder (purity >99.9%) obtained from the Wako Pure Chemical Co. The BET surface area of the sample was 14.1 $m^2\ g^{-1}$ which did not change after repeated reduction-oxidation cycles. Water was purified three times by trap-to-trap distillation in a vacuum apparatus. The ^{18}O-labelled oxygen gas was obtained from the Atomic Energy commissariat (France). The $H_2{}^{18}O$ was prepared by the reaction of H_2 with $^{18}O_2$. D_2 was obtained from the Takachiho Chemical Co. Reduction of CeO_2 to a desired average ratio of O/Ce was carried out at 873–973 K using hydrogen.

Kinetic Measurements

Kinetic measurements were carried out using a conventional mercury-free gas-circulation apparatus of *ca.* 334 cm^3 volume, capable of achieving a vacuum to 1.3×10^{-4} Pa. Oxidation of the reduced cerium oxide (CeO_y, y is average O/Ce ratio of the sample) was initiated by adding and circulating water vapor (2.1 kPa was kept during the reaction by vapor saturation of water at 291 K). The quantity of the hydrogen produced was analyzed by gas-chromatography at appropriate time intervals. The oxidation with oxygen gas was followed by measuring the decrease of pressure of oxygen.

The exchange of oxygen between $H_2{}^{18}O$ and CeO_y was measured by analyzing oxygen-isotope compositions in the gas phase using a quadrupole mass spectrometer.

Results and Discussion

Effect of the Average Ratio of O/Ce on the Rate of Water-Decomposition

The kinetics of hydrogen formation accompanied by reoxidation of the CeO_y (y, average O/Ce ratio) with water vapor were measured at 573 K for the samples with different initial ratios of O/Ce. The changes in the composition of the samples with time were calculated on the basis of the quantity of hydrogen produced, *i.e.*, the corresponding quantity of oxygen was assumed to be transferred into the oxygen vacancies of the cerium oxide homogeneously. Figure 2 represents the kinetic curves of oxidation thus obtained. The results in Fig. 2 show that the oxidation seems to cease at a composition of $y = 1.993 \pm 0.003$. However, when the temperature was raised to 773 K, the reaction proceeded further to completion ($y = 2.000$) within the experimental error of ± 0.003 in y. Ban and Nowick reported a similar observation in the case of oxidation by oxygen [15]. As they suggested, it is probable that the low temperature-reoxidized cerium oxide may first come back to a metastable material called α' which then returns to the original stoichiometric CeO_2(α-phase) at high temperatures >623 K. Figure 3 shows the effect of the composition of CeO_y

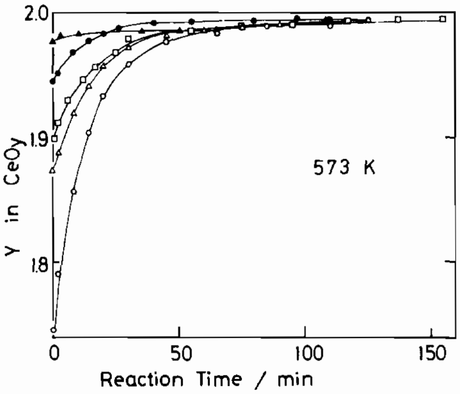

Fig. 2. Kinetic curves of oxidation for various starting compositions of CeO_y: at 573 K.

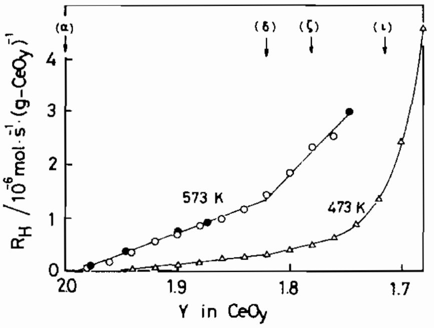

Fig. 3. Rates of hydrogen formation (R_H) as functions of y in CeO_y: at 573 and 473 K.

on the rates of hydrogen production. The rates were calculated from the slopes of the kinetic curves. The rates are normalized to the quantity of hydrogen produced per second per gram of CeO_2. The closed circles are the initial rates for the samples demonstrated in Fig. 2. The open circles are the rates measured from the slopes of the kinetic curves at corresponding values of y for the sample of starting composition of $CeO_{1.747}$. The fact that the open and closed circles are on the same line suggests that the phase reaction proceeds consecutively, *i.e.*, $\iota \rightarrow \zeta \rightarrow \delta \rightarrow \alpha'$. The triangles are the plot for the starting composition of $CeO_{1.614}$. Although the reaction was carried out at 473 K, the initial rate for the sample was too fast to be measured accurately. Therefore, only the rates for the y larger than 1.680 are plotted in the figure. The sudden increases in the rates above the O/Ce ratio of 1.82, which can be observed for the two curves in Fig. 3, must be ascribed to the appearance of ζ, ι or θ phase according to the composition of CeO_y. Although the difference in reactivities among these phases is of interest, the present work will be focused only on the reaction between the δ-phase and water vapor. The linear correlation between the rate and the composition of CeO_y ($y < 1.82$) observed for the data at 573 K shows that the rate is proportional to the concentration of the δ-phase.

Temperature Effect on the Rate of Water Decomposition

The kinetics of water decomposition of the starting composition of $CeO_{1.900 \pm 0.003}$ were observed at temperatures 298 to 598 K. Figure 4 represents the Arrhenius plot of the initial rates of hydrogen formation. The plot shows two lines having different slopes. The slopes of the lines give apparent activation energies of 33.4 and 18.1 kJ mol^{-1} for the temperature ranges below and above 453 K, respectively. This result suggests that the rate-determining step of the reaction at low temperatures differs from that at high temperatures.

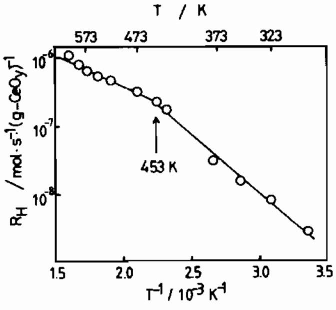

Fig. 4. Rate of hydrogen formation (R_H) as a function of temperature: starting composition $CeO_{1.900}$.

Pressure Effect on the Rate of Water Decomposition

The effect of vapor pressure of water on the rate of hydrogen formation was examined at two different temperatures below and above 453 K. The experiments were carried out at 373 and 523 K using a sample of starting composition of $CeO_{1.900}$. The initial rates observed at the two temperatures were plotted in Fig. 5 as functions of vapor pressure of water. Figure 5 shows that the rates at 373 K are proportional to the pressure. On the other hand, the rates at 523 K are proportional to the square root of water pressure as indicated in Fig. 6. The different pressure dependences of the rates observed between the two temperatures can not be ascribed to the change in adsorption coverage of water because the pressure dependence of the coverage is usually greater at high temperatures than at lower temperatures. The different orders of pressure in kinetic equations observed at the two temperatures support the idea that the rate-determining steps between the two temperatures are different.

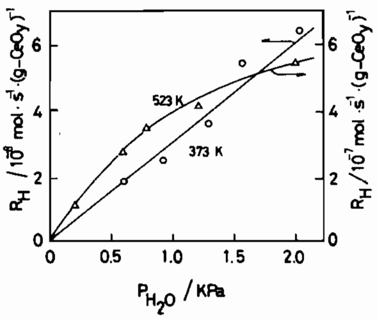

Fig. 5. Effects of vapor pressure of water on the rates of hydrogen formation at 373 and 523 K: starting composition $CeO_{1.900}$.

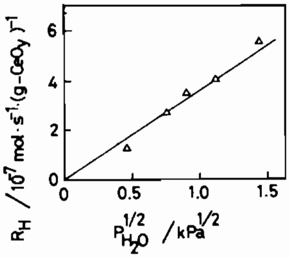

Fig. 6. Relation between the rate of hydrogen formation and $(P_{H_2O})^{1/2}$ at 523 K.

Oxygen Exchange between $H_2{}^{18}O$ and Cerium Oxide

The oxygen exchanges between $H_2{}^{18}O$ and $CeO_{1.900}$ or CeO_2 were observed at low temperatures.

The initial quantity of water vapor added to the system was 9.4×10^{-5} mol which corresponded to 8.5 and 8.1% of the quantities of lattice oxygen in $CeO_{1.900}$ and CeO_2 (0.10 g) used for the experiments, respectively. Figure 7 shows the time course of the decrease in the mole fraction of $H_2{}^{18}O$ according to the progress of the exchange at the temperatures indicated in the figure. The exchange between $H_2{}^{18}O$ and CeO_2 did not occur at 298 K but proceeded slowly above 373 K. On the other hand, the exchange reaction for the initial composition of $CeO_{1.900}$ took place rapidly at 298 K. The rate of this exchange is more than two orders of magnitude greater than that of decomposition of water at the same temperature. This fact strongly suggests that the dissociation of water and the exchange of the oxygen atom of water with lattice oxygen proceed rapidly before the reduction of water by Ce^{3+}. The faster oxygen exchange for $CeO_{1.900}$ compared with CeO_2 observed in Fig. 7 can be ascribed to the greater number of anion vacancies for the former sample compared to the latter.

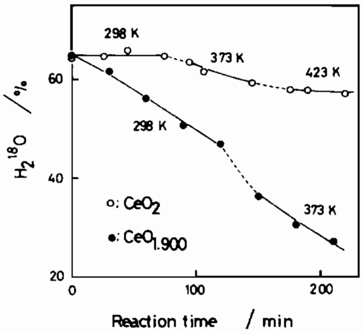

Fig. 7. Oxygen-exchange between $H_2{}^{18}O$ and cerium oxide (CeO_2 and starting composition $CeO_{1.900}$) at the temperatures indicated in the figure.

The reaction scheme for oxygen-exchange which we have in mind is demonstrated in Fig. 8. The water molecule dissociatively adsorbs on oxygen ion vacancies (□) and lattice oxygen ions (O_l) (step *i*). The switch between the oxygen vacancy and the lattice oxygen occurs on step *ii*, which results in the exchange of oxygen between water and cerium oxides (step *iii*).

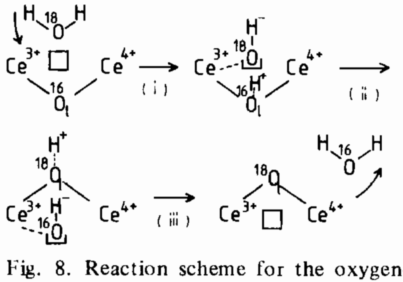

Fig. 8. Reaction scheme for the oxygen-exchange between $H_2{}^{18}O$ and CeO_y.

Hydrogen Exchange for the Systems H_2–D_2 and H_2O–D_2 over $CeO_{1.900}$

H_2–D_2 exchange was carried out over $CeO_{1.900}$ under a pressure of 6.7 kPa ($H_2/D_2 = 1.00$). The reaction proceeded rapidly at 373 K. The exchange of hydrogen between H_2O (2.3×10^{-4} mol) and D_2 (4.5×10^{-4} mol) was also examined over the starting composition of $CeO_{1.900}$ at 373 K. The decomposition of H_2O proceeded at this temperature, but H_2O–D_2 exchange did not take place at all. These results show that, although both hydrogen and water can be activated at 373 K, the hydrogen mixing between them is not allowed.

Reaction Scheme of Water Decomposition

Let us consider the probable elementary steps for the reaction between water and δ-phase cerium oxide. As described earlier, the rapid oxygen exchange between H_2O^{18} and $CeO_{1.900}$ (Fig. 7) suggests that the water molecule is dissociatively coordinated to Ce^{3+} and lattice oxygen ions on the surface. Moreover, the coordination and the oxygen exchange occur rapidly and reversibly compared to the rate of hydrogen formation, indicating that neither the adsorption of water molecules nor the diffusion of oxygen ions in the bulk can be rate-determining steps. Thus, let us assume first the equilibrium coordination of water as represented by eqn. 1 in Fig. 9, where Ce^{3+} (a) and Ce^{3+} (b) are the six- and seven-coordinated Ce^{3+} ions, respectively, which are present in the nonstoichiometric cerium oxide of fluorite-based structure. □ represents an oxygen ion vacancy. O_L is the oxygen ion bridging Ce^{3+} (a) and Ce^{3+} (b). The OH^- may be coordinated to Ce^{3+} (a) through the position of oxygen-ion vacancy. The OH^- is reduced by Ce^{3+} (a) in step 2. The H^+ formed by dissociative adsorption of H_2O in step 1 is subsequently reduced by Ce^{3+} (b), pro-

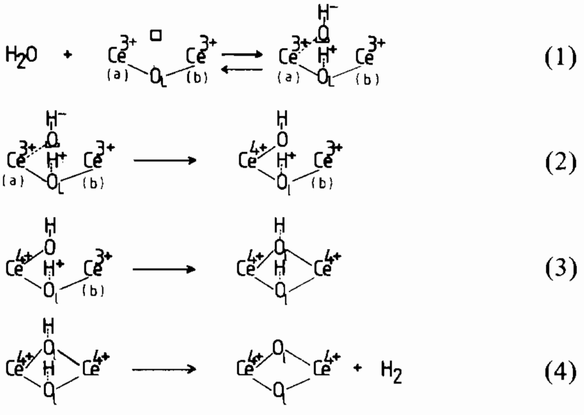

Fig. 9. Reaction scheme of water-decomposition.

ducing hydrogen atoms and lattice oxygen-ions in step **3**. The hydrogen atoms recombine and desorb to the gas phase in step **4**. The kinetic studies described earlier suggested that the rate-determining step of the overall reaction is different for the temperatures above and below 453 K. Assuming that the concentrations of OH^- and H^+ on the surface are equal and can be expressed by Henry's law, the rate of hydrogen formation (R_H) is written by eqn. 5 when step **2** is rate-determining.

$$R_H = k_2 N_{OH^-} = k_2(K_1 P_{H_2O} N_\Box N_{O_L})^{1/2} \qquad (5)$$

where, N_{OH^-}, $N_\Box$, N_{O_L} are the numbers of OH^-, oxygen ion vacancies on the basis of fluorite structure, and lattice oxygen ions, respectively, on the surface of cerium oxide samples. For a fixed composition of CeO_y, $N_\Box$ and N_{O_L} are constant. Moreover the ratio $N_{O_L}/N_\Box$ is three since pairs of oxygen vacancies are believed to be along the ⟨111⟩ axis of the original fluorite structure [6]. Hence, R_H is given as follows:

$$R_H = k_{II} P_{H_2O}{}^{1/2} \qquad (6)$$

where, $k_{II} = k_2(3K_1)^{1/2} N_\Box$. If step **3** is rate-determining, R_H can likewise be written as follows:

$$R_H = k_3 N_{O_LH} N_{H^+} = k_3 K_2 N_{OH^-} N_{H^+}$$
$$= k_3 K_2 K_1 N_\Box N_{O_L} P_{H_2O} \qquad (7)$$

where N_{O_LH} and N_{H^+} are the numbers of O_L–H and H^+, respecitvely. K_2 is the equilibrium constant for step **2**. For a fixed composition of CeO_y:

$$R_H = k_{III} P_{H_2O} \qquad (8)$$

where $k_{III} = 3k_3 K_1 K_2 N_\Box{}^2$. When recombination of hydrogen atoms (step **4**) is rate-determining, the rate equation is given by:

$$R_H = k_4 N_H{}^2 = k_4 K_1 K_2 K_3 N_\Box N_{O_L} P_{H_2O} \qquad (9)$$

For a fixed composition of CeO_y:

$$R_H = k_{IV} P_{H_2O} \qquad (10)$$

where $k_{IV} = 3k_4 K_1 K_2 K_3 N_\Box{}^2$. The kinetic equation observed for the reaction at 373 K (which was in the low temperature range) was first order with respect to the pressure of water vapor (Fig. 5). This result suggests that the rate-determining step is either step **3** or **4**. As described earlier the hydrogen exchange between H_2 and D_2 occurred rapidly at 373 K which was in the low temperature range. This fact implies that the recombination of hydrogen atoms (step **4**) is not rate-determining. The absence of hydrogen exchange between H_2O and D_2 can be explained when step **3** is rate-determining. Therefore, the kinetic studies conclude that step **3** is the most probable rate-determining step at low temperatures (<453 K). The kinetic equation obtained at 523 K (which is in the high temperature range) is in accord with eqn. 6. The linear increase in the rate of hydrogen-production with the decrease in y of CeO_y (Fig. 3) is also explained by eqn. 6 which requires proportional correlation between the rate and the quantity of oxygen vacancies. Thus, we believe that the rate-determining step at high temperatures (>453 K) is step **2** in Fig. 9.

References

1 P. B. Tarman and R. Bijentina, *Coal Proc. Technol.*, *5*, 114 (1979).
2 S. Nakaguchi, *J. Jpn. Petrol. Inst.*, *20*, 69 (1977).
3 Y. Murakami, A. Miyamoto, S. Kamitomai, K. Kurahashi and Y. Kosaki, *J. Jpn. Petrol. Inst.*, *25*, 380 (1982).
4 K. Otsuka, S. Murakoshi and A. Morikawa, *Fuel Proc. Technol.*, *7*, 203 (1983).
5 K. Otsuka, M. Hatano and A. Morikawa, *J. Catal.*, *79*, 493 (1983).
6 B. G. Hyde and L. Eyring, in L. Eyring (ed.), 'Rare Earth Research III', Gordon and Breach, New York, 1965, p. 623.
7 J. O. Sawyer, B. G. Hyde and L. Eyring, *Bull. Soc. Chim. Fr.*, 1190 (1965).
8 D. J. M. Bevan and J. Kordis, *J. Inorg. Nucl. Chem.*, *26*, 1509 (1964).
9 S. P. Ray and A. S. Nowick, *J. Solid State Chem.*, *15*, 344 (1975).
10 U. E. Kuntz and L. Eyring, in W. D. Kingery (ed.), 'Kinetics of High-temperature Processes', Wiley, New York, 1959, p. 50.
11 S. P. Ray and A. S. Nowick, in A. R. Cooper and A. H. Hener (eds.), 'Mass Transport Phenomena in Ceramics', Plenum, New York, 1975, p. 187.
12 T. H. Estell and S. N. Flengas, *Chem. Rev.*, *70*, 339 (1970).
13 H. Inaba, S. P. Pack, S. H. Lin and L. Eyring, *J. Solid State Chem.*, *33*, 295 (1980).
14 T. Sugihara, S. H. Lin and L. Eyring, *J. Solid State Chem.*, *40*, 226 (1981).
15 Y. Ban and A. S. Nowick, in 'Proceedings of 5th Materials Research Symposium, Vol. 364', NBS Special Publ., 1972, p. 353.